The $TeOF_6^{2-}$ Anion: The First Example of a Multiply Charged, Pentagonal Bipyramidal, Main-Group Element AX_5YZ Species and the Vibrational Spectra of the $TeOF_5^-$ Anion

Karl O. Christe,*,† David A. Dixon,‡ Jeremy C. P. Sanders,§ Gary J. Schrobilgen,*,§ and William W. Wilson†

Rocketdyne, A Division of Rockwell International, Canoga Park, California 91309, Department of Chemistry, McMaster University, Hamilton, Ontario L8S 4MI, Canada, and Central Research and Development Department, E. I. du Pont de Nemours and Company, Inc., Experimental Station, Wilmington, Delaware 19880-0328

Received May 21, 1993

The new $TeOF_6^{2-}$ anion has been isolated in the form of its tetramethylammonium salt from solutions of $N(CH_3)_4F$ and $N(CH_3)_4TeOF_5$ in CH_3CN. It was characterized by vibrational spectroscopy, a normal coordinate analysis and ab initio calculations. It is shown that its structure is analogous to that of the recently discovered, isoelectronic IOF_6^- anion which makes it only the second known representative of a pentagonal bipyramidal, main-group element AX_5YZ species and the first multiply charged example of such a species. The stretching force constant of the TeF_5 part of $TeOF_6^{2-}$ is significantly smaller than that in IOF_6^- indicating that the additional negative charge in $TeOF_6^{2-}$ weakens mainly the equatorial Te–F bonds. The vibrational spectra of $N(CH_3)_4TeOF_5$ are also reported, and the results of ab initio calculations and of a normal coordinate analysis of $TeOF_5^-$ show that six of its fundamental vibrations had previously been assigned incorrectly.

Introduction

Heptacoordinated species are of special interest. According to the hard sphere model of the valence shell electron pair repulsion (VSEPR) rules of repelling points on a sphere, heptacoordinated species should prefer structures derived from a monocapped octahedron.[1,2] Besides the monocapped octahedron, there are two other structures for heptacoordinated species that are only slightly higher in energy. These are the monocapped trigonal prism and the pentagonal bipyramid.[3] Examinations[4,5] of the relative energy E of seven repelling points on a sphere in terms of the energy law

$$E = \sum_{i \neq j} \frac{1}{r_{ij}^{\,n}}$$

where r_{ij} is the distance between two of the points and n is a constant, have indicated that for heptacoordinated species the minimum energy structure depends on n. For $0 < n < 3$, i.e., soft repulsion, the pentagonal bipyramid was the minimum energy structure, while for $3 < n < 6$ the monocapped trigonal prism and for $n > 6$, i.e., hard repulsion, the monocapped octahedron were the energetically preferred structures.[5] Although at present no quantitative numbers are available[2] for n, for heptacoordinated transition metal fluorides or oxofluorides the experimental observations qualitatively agree with these predictions. Thus, the most ionic and softest XF_7 or XOF_6 species, i.e., the triply charged anions ZrF_7^{3-}, HfF_7^{3-}, $TaOF_6^{3-}$, and $NbOF_6^{3-}$ have pentagonal bipyramidal structures,[2,6,7] the intermediately soft, doubly charged anions NbF_7^{2-} and TaF_7^{2-} have monocapped trigonal prismatic structures,[8,9] and the hardest, singly charged anions MoF_7^-, WF_7^-, and UF_7^- possess monocapped octahedral structures.[10] On the basis of the presently available structural data, the nature of the central atom or small changes in its d orbital occupation seem to have little influence on the structures of these compounds.

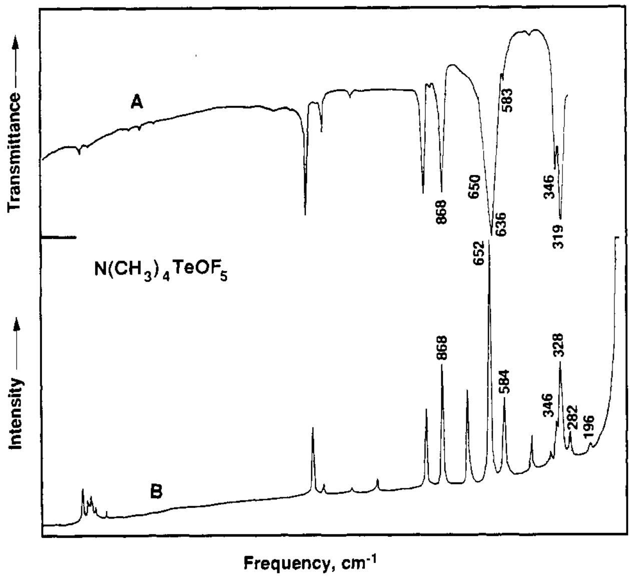

Figure 1. Infrared (A) and Raman (B) spectra of solid $N(CH_3)_4TeOF_5$.

Whereas the aforementioned VSEPR rules and energy law predictions[5] appear to be applicable to transition metal elements, the heptacoordinated main-group elements do not comply. By comparison with identically charged transition metal compounds, the heptacoordinated main-group compounds should be even harder because of the smaller radii of their central atoms and the increased s and p character of their valence electrons. Therefore, the neutral or singly charged heptacoordinated main-group

---

† Rocketdyne.

‡ DuPont.

§ McMaster University.

(1) Gillespie, R. J. *Molecular Geometry*; Van Nostrand Reinhold Co.: London, 1972.

(2) Gillespie, R. J.; Hargittai, I. *The VSEPR Model of Molecular Geometry*; Allyn and Bacon, A Division of Simon & Schuster, Inc.: Needham Heights, MA, 1991.

(3) Kepert, D. *Inorganic Stereochemistry*; Springer: Berlin, 1982.

(4) Claxton, T. A.; Benson, G. C. *Can. J. Chem.* **1966**, *44*, 157.

(5) Bradford Thompson, H.; Bartell, L. S. *Inorg. Chem.* **1968**, *7*, 488.

(6) Granzin, J.; Saalfeld, H. *Z. Kristallogr.* **1988**, *183*, 71.

(7) (a) Averdunk, F.; Hoppe, R. *J. Fluorine Chem.* **1989**, *42*, 413. (b) Stomberg, R. *Acta Chem. Scand., Ser. A* **1983**, *A37*, 412.

(8) Torardi, C. C.; Brixner, L. H.; Blasse, G. *J. Solid State Chem.* **1987**, *67*, 21.

(9) Brown, G. M.; Walker, L. A. *Acta Crystallogr.* **1966**, *20*, 220.

(10) Giese, S.; Seppelt, K. *J. Fluorine Chem.* **1992**, *58*, 368.

0020-1669/93/1332-4089$04.00/0

Table I. Vibrational Spectra of $N(CH_3)_4TeOF_5$ and Their Assignments

obsd freq, cm^{-1} (rel intens)			assignments (point group)	
	Raman			
IR 25 °C	25 °C	−150 °C	$N(CH_3)_4^+$ (T_d)	$TeOF_5^-$ (C_{4v})
3110 sh	3043 (13)	3045 (8)	ν_5 (E) ν_{14} (F_2) ν_1 (A_1) + combination bands	
3042 mw	2995 (7)	3030 (7)		
	2966 (10)	2968 (2)		
2972 w	2928 (w)			
	2820 (3)	2931 (2)		
		2820 (3)		
2759 vw				
2660 vvw				
2622 vvw				
2588 vw				
2523 vvw				
2485 vw				
2362 vvw				
1492 vs			ν_{15} (F_2)	
	1465 (26)	1477 (10)	ν_2 (A_1), ν_6 (E)	
		1465 (7)		
1419 m	1418 (5)	1421 (2)	ν_{16} (F_2)	
1289 mw	1289 (2)	1288 (1)	ν_{17} (F_2)	
1220 w				(584 + 636)
	1174 (5)	1175 (1)	ν_7 (E)	
951 s	949 (28)	952 (18)	ν_{18} (F_2)	
921 w				
868 s	868 (47)	858 (35)		ν_1 (A_1)
828 vw, sh				
770 w				
	753 (37)	758 (12)	ν_3 (A_1)	
	742sh	748 (7)		
650 sh	652 (100)	652 (100)		ν_2 (A_1)
636 vs				ν_8 (E)
583 mw	584 (30)	594 (22)		ν_3 (A_1), ν_5 (B_1)
460 w	460 (13)	459 (7)	ν_{19} (F_2)	
	373 (5)	375 (4)	ν_8 (E)	
346 ms	346 (6)	347 (9)		ν_9 (E)
329 sh	328 (40)	329 (40)		ν_{10} (E)
319 s				ν_4 (A_1)
	282 (10)	283 (6)		ν_7 (B_2)
	196 (3)	196 (3)		ν_{11} (E)
		93 (2)	lattice vibrations	
		38 (2)		

element compounds should be very hard and exhibit monocapped octahedral structures. This, however, is not the case, and IF_7,[11,12] TeF_7^-,[13,14] IOF_6^-,[13,15] and XeF_5^- [16] all exhibit pentagonal bipyramidal structures. A rationale for their structures was recently presented in our papers on IF_7[12] and IOF_6^-.[15] It was concluded[12,15] that the pentagonal bipyramidal geometry of their more localized valence electron orbitals, rather than the intramolecular repulsion force, is the main reason for their pentagonal bipyramidal molecular structures.

The bonding in the pentagonal bipyramidal main-group fluorides has been described[12,15] by planar, $p_{x,y}$ hybrid orbitals of the central atom for the formation of a coplanar, semiionic, 6-center–10-electron (6c–10e) bond system for the five equatorial ligands. Depending on the relative bond lengths and radii of the atoms involved, this equatorial plane can become highly congested and, therefore, undergo substantial puckering. Further interest and complexity is added to this problem by the facts that these structures possess 5-fold symmetry, are usually nonrigid, and exhibit fluxionality involving static or dynamic puckering of the equatorial plane and, in some instances,[12] also axial–equatorial ligand exchange.

In view of the strong dependency of the structures of the heptacoordinated transition metal compounds upon the number of their ionic charges, (see above) it was interesting to explore to what extend this also applies to heptacoordinated main-group element compounds. Whereas neutral IF_7 and the singly charged anions TeF_7^-, IOF_6^-, and XeF_5^- are now well understood,[11,16] no data had been available on multiply charged anions. Therefore, we have prepared and characterized the $TeOF_6^{2-}$ anion and, in this paper, report our results.

Experimental Section

Materials. The synthesis of anhydrous $N(CH_3)_4F$ has been previously described.[17] The CH_3CN (Baker, Bio-analyzed, having a water content of 40 ppm) was treated with P_2O_5 and freshly distilled prior to use, thereby reducing its water content to <4 ppm. A literature method[18] was used for the synthesis of anhydrous $N(CH_3)_4TeOF_5$.

Synthesis of $[N(CH_3)_4]_2TeOF_6$. In the drybox, $N(CH_3)_4TeOF_5$ (0.4543 g, 1.45 mmol) and a 2-fold excess of $N(CH_3)_4F$ (0.2726 g, 2.93 mmol) were loaded into separate limbs of a two-limbed Pyrex glass vessel equipped with J. Young glass–PTFE stopcocks. Dry CH_3CN (ca. 5 mL of liquid) was vacuum distilled onto each solid at −196 °C. The two limbs were allowed to warm to −9 °C in order to dissolve the solids. While both solutions were maintained at −9 °C, the $N(CH_3)_4F$ solution was poured into the $N(CH_3)_4TeOF_5$ solution. The reaction mixture was stirred at −9 °C for 15 min, during which time a heavy white precipitate formed. The mixture was cooled to −20 °C and stirred for an additional 45 min. The supernatant solution was decanted from the white precipitate at −20 °C. The residual CH_3CN was pumped off at −9 °C and finally at 25 °C overnight. A fine white powder remained (0.4298 g), which was shown by Raman and infrared spectroscopy to be a mixture of $[N(CH_3)_4]_2TeOF_6$ and $N(CH_3)_4TeOF_5$.

Vibrational Spectroscopy. Raman spectra were recorded on either a Cary Model 83 or a Spex Model 1403 spectrophotometer using the 488-nm exciting line of an Ar ion or the 647.1-nm line of a Kr ion laser, respectively. Baked-out Pyrex melting point capillaries or thin-walled Kel-F tubes were used as sample containers.

Infrared spectra were recorded by using either AgCl, AgBr, or KBr disks on a Perkin-Elmer Model 283 spectrophotometer. The finely powdered samples were sandwiched between two thin disks and pressed together in a Wilks minipress inside the drybox.

Nuclear Magnetic Resonance Spectroscopy. The ^{19}F NMR spectra were recorded unlocked (field drift <0.1 Hz h^{-1}) on a Bruker AM-500 spectrometer equipped with an 11.744-T cryomagnet. The ^{19}F spectra were obtained using a 5-mm combination $^1H/^{19}F$ probe operating at 470.599 MHz. The spectra were recorded in a 32 K memory. A spectral width setting of 50 kHz was employed, yielding a data point resolution of 3.052 Hz/data point and an acquisition time of 0.327 s. No relaxation delays were applied. Typically, 10 000 transients were accumulated. The pulse width corresponding to a bulk magnetization tip angle, θ, of approximately 90° was equal to 1 μs. No line broadening parameters were used in the exponential multiplication of the free induction decays prior to Fourier transformation.

The spectra were referenced to a neat external sample of $CFCl_3$ at ambient temperature. The chemical shift convention used is that a positive (negative) sign signifies a chemical shift to high (low) frequency of the reference compound.

Solids were weighed into 5-mm precision glass tubes (Wilmad) in the drybox, and CH_3CN solvent was distilled *in vacuo* onto the solid at −78 °C. The tubes were flame-sealed in dynamic vacuum while keeping the contents frozen to −78 °C.

Computational Methods. The electronic structure calculations were done at the ab initio molecular orbital level using an effective core potential (ECP) for the core electrons on tellurium. The valence basis set is of polarized double zeta quality. The fluorine and oxygen basis sets are

---

(11) Adams, W. J.; Bradford Thompson, H.; Bartell, L. S. *J. Chem. Phys.* **1970**, *53*, 4040.

(12) Christe, K. O.; Curtis, E. C.; Dixon, D. A. *J. Am. Chem. Soc.*, in press.

(13) Christe, K. O.; Sanders, J. C. P.; Schrobilgen, G. J.; Wilson, W. W. *J. Chem. Soc., Chem. Commun.* **1991**, 837.

(14) Mahjoub, A. R.; Seppelt, K. *J. Chem. Soc., Chem. Commun.* **1991**, 840.

(15) Christe, K. O.; Dixon, D. A.; Mahjoub, A. R.; Mercier, H. P. A.; Sanders, J. C. P.; Seppelt, K.; Schrobilgen, G. J.; Wilson, W. W. *J. Am. Chem. Soc.*, in press.

(16) Christe, K. O.; Curtis, E. C.; Dixon, D. A.; Mercier, H. P.; Sanders, J. C. P.; Schrobilgen, G. J. *J. Am. Chem. Soc.* **1991**, *113*, 3351.

(17) Christe, K. O.; Wilson, W. W.; Wilson, R. D.; Bau, R.; Feng, J. *J. Am. Chem. Soc.* **1990**, *112*, 7619.

(18) Mercier, H. P. A.; Sanders, J. C. P.; Schrobilgen, G. J. *J. Am. Chem. Soc.*, submitted for publication.

Table II. Observed and Calculated Vibrational Spectra of $TeOF_5^-$

assignment C_{4v}		approx mode description	obsd			calcd		
			freq, cm^{-1} (rel intens)		$^{16}O-^{18}O$ shift[a]	freq,[b] cm^{-1}	IR intens	$^{16}O-^{18}O$ shift
			IR	Raman				
A$_1$	ν_1	ν(TeO)	868 s	868 (47)	40	860	101	39.9
	ν_2	sym combination of $\nu_{sym}(TeF_4)$ and $\nu(TeF_{ax})$	650 sh	652 (100)	1	658	63	1.5
	ν_3	antisym combination of $\nu_{sym}(TeF_4)$ and $\nu(TeF_{ax})$	583 mw	584 (30)	0	573	3	0.3
	ν_4	$\delta_{umbrella}(TeF_4)$	319 s			339	106	0.8
B$_1$	ν_5	$\nu_{sym}(TeF_4)$ out-of-phase		584 (30)		582	0	0
	ν_6	$\delta_{pucker}(TeF_4)$	not obsd	not obsd		223	0	0
B$_2$	ν_7	$\delta_{sciss}(TeF_4)$ in-plane		282 (10)	0	280	0	0
E	ν_8	$\nu_{asym}(TeF_4)$	636 ms		0	651	221	0
	ν_9	$\delta(FTeF_4)$	346 ms	346 (6)	0	348	61	0.2
	ν_{10}	$\delta(OTeF_4)$	329 sh	328 (40)	10	329	60	10.2
	ν_{11}	$\delta_{asym}(TeF_4)$ in-plane		196 (3)		185	0.04	1.9

[a] The oxygen isotopic shift data were taken from ref 32. [b] The calculated frequencies were scaled by the following empirical factors to give the best agreement with the observed values: stretching frequencies, 0.9529; deformation modes, 0.8812.

Table III. Observed and Calculated Geometries of $TeOF_5^-$

	obsd[a]	calcd[b]		obsd[a]	calcd[b]
r(Te–O), Å	1.786(3)	1.738	r(Te–F$_{eq}$), Å	1.853(2)	1.838
r(Te–F$_{ax}$), Å	1.854(2)	1.835	∠(OTeF$_{eq}$), deg	95.2(1)	97.44

[a] Librationally uncorrected values reported in ref 32 for the solid $TeOF_5^-$ salt of protonated 1,8-bis(dimethylamino)naphthalene at −106 °C. [b] Unscaled values calculated for the free $TeOF_5^-$ anion.

Table IV. Ab Initio Force Field[a,b] of $TeOF_5^-$ and Potential Energy Distribution

			sym force consts	PED
A$_1$	ν_1	860	$F_{11} = f_D = 6.164$	92.3 (S_1) + 4.1 (S_2) + 3.3 (S_4)
			$F_{12} = f_{DR} = 0.028$	
			$F_{13} = f_{Dr} = 0.137$	
			$F_{14} = 0.198$	
	ν_2	658	$F_{22} = f_R = 3.929$	52.8 (S_2) + 44.9 (S_3) + 1.2 (S_4) + 1.1 (S_1)
			$F_{23} = f_{Rr} = 0.448$	
			$F_{24} = -0.505$	
	ν_3	573	$F_{33} = f_r + 2f_{rr} + f_{rr'} = 4.179$	50.3 (S_3) + 49.3 (S_2)
			$F_{34} = -0.027$	
	ν_4	339	$F_{44} = 1.514$	98.8 (S_4) + 1.0 (S_2)
B$_1$	ν_5	282	$F_{55} = f_r - 2f_{rr} + f_{rr'} = 3.782$	100 (S_5)
			$F_{56} = 0.027$	
	ν_6	223	$F_{66} = 0.942$	100 (S_6)
B$_2$	ν_7	280	$F_{77} = f_\alpha - 2f_{\alpha\alpha} + f_{\alpha\alpha'} = 0.755$	100 (S_7)
E	ν_8	651	$F_{88} = f_r - f_{rr'} = 3.789$	94.8 (S_8) + 2.7 (S_{11}) + 2.0 (S_{10})
			$F_{89} = f_{r\beta} - f_{r\beta''} = 0.343$	
			$F_{8,10} = f_{r\gamma} - f_{r\gamma''} = 0.242$	
			$F_{8,11} = 2^{1/2}(f_{r\alpha} - f_{r\alpha'}) = 0.141$	
	ν_9	348	$F_{99} = f_\beta - f_{\beta\beta'} = 1.262$	78.1 (S_9) + 21.6 (S_{11})
			$F_{9,10} = 0.088$	
			$F_{9,11} = 0.182$	
	ν_{10}	329	$F_{10,10} = f_\gamma - f_{\gamma\gamma'} = 0.919$	86.0 (S_{10}) + 7.1 (S_9) + 6.9 (S_{11})
			$F_{10,11} = 0.188$	
	ν_{11}	185	$F_{11,11} = f_\alpha - f_{\alpha\alpha'} = 0.865$	67.1 (S_{11}) + 20.1 (S_{10}) + 12.6 (S_9)

[a] The following symmetry coordinates were used: S_1 = TeO stretch; S_2 = TeF$_{ax}$ stretch; S_3 = TeF$_4$ sym in-phase stretch; S_4 = TeF$_4$ unbrella deform; S_5 = TeF$_4$ sym out-of-phase stretch; S_6 = TeF$_4$ pucker deform; S_7 = TeF$_4$ sym in-plane deform; S_8 = TeF$_4$ asym stretch; S_9 = TeF$_{ax}$ wag; S_{10} = TeO wag; S_{11} = TeF$_4$ asym in-plane deform. For their explicit values, see: Smith, D. F.; Begun, G. M. *J. Chem. Phys.* **1965**, *43*, 2001. [b] The following scaling factors were used: stretching force constants, $(0.9529)^2$; deformation constants, $(0.8812)^2$; stretch–bend interactions, 0.9529 × 0.8812. Stretching constants are in mdyn/Å, deformation constants in mdyn Å/rad^2, and stretch–bend interaction constants in mdyn/rad.

Table V. Vibrational Spectra of $[N(CH_3)_4]_2TeOF_6$ and Their Assignment

obsd freq (25 °C), cm^{-1} (rel intens)		assignment (point group)	
IR	Ra	$N(CH_3)_4^+$ (T_d)	$TeOF_6^{2-}$ (C_{5v})
3043 mw	3036 (40)	ν_5 (E) ν_{14} (F$_2$) ν_1 (A$_1$) + combination bands	
2999 w	2996 (5)		
	2968 (30)		
	2945 sh		
	2928 (20)		
	2900 sh		
	2825 (9)		
1498 vs		ν_{15} (F$_2$)	
1464 w	1474 (91)	ν_2 (A$_2$), ν_6 (E)	
1421 w	1420 (9)	ν_{16} (F$_2$)	
	1291 (9)	ν_{17} (F$_2$)	
	1185 (9)	ν_7 (E)	
954 vs	952 (72)	ν_{18} (F$_2$)	
921 w	919 (10)		
830 s	830 (71)		ν_1 (A$_1$)
	752 (80)	ν_3 (A$_1$)	
614 m	614 (100)		ν_2 (A$_1$)
	530 (63)		ν_3 (A$_1$)
525 vs			ν_5 (E$_1$)
461 w	459 (25)	ν_{19} (F$_2$)	ν_9 (E$_2$)?
	388 (35)		ν_{10} (E$_2$)
	368 sh	ν_8 (E)	
365 vs			ν_6 (E$_1$)
330 s			ν_4 (A$_1$)
	322 (60)		ν_7 (E$_1$)
	245 (2)		ν_8 (E$_1$)

from Dunning and Hay,[19] and the ECP is from Hay and Wadt[20] including relativistic corrections and augmented by a d function on Te with an exponent of 0.237.[21] The Te, O, and F basis sets were augmented further by a diffuse p function with exponents of 0.035, 0.059, and 0.074, respectively, to account for the negative ion character. The geometries were optimized by using gradient techniques,[22] and the force fields were calculated analytically.[23,24] The ab initio MO calculations were done with the program GRADSCF,[25] as implemented on a Cray YMP computer system. Because the calculated vibrational frequencies and force constants are somewhat too high due to the neglect of electron correlation and of anharmonicity, the calculated frequencies and force constants require scaling. Since the deformation modes are usually more strongly affected

---

(19) Dunning, T. H., Jr.; Hay, P. J. In *Methods of Electronic Structure Theory*, Schaefer, H. F., III, Ed., Plenum Press: New York, 1977; Chapter 1.

(20) Hay, P. J.; Wadt, W. R. *J. Chem. Phys.* **1985**, *82*, 299.

(21) Huzinaga, S.; Andzelm, J.; Klobukowski, M.; Radzio, E.; Sakai, Y.; Tatasaki, H. *Gaussian Basis Sets of Molecular Calculations*; Elsevier: Amsterdam, 1984.

(22) (a) Komornicki, A.; Ishida, K.; Morokuma, K.; Ditchfield, R.; Conrad, M. *Chem. Phys. Lett.* **1977**, *45*, 595. (b) McIver, J. W., Jr.; Komornicki, A. *Chem. Phys. Lett.* **1971**, *10*, 202. (c) Pulay, P. In *Applications of Electronic Structure Theory*, Schaefer, H. F., III, Ed.; Plenum Press: New York, 1977; p 153.

(23) (a) King, H. F.; Komornicki, A. *J. Chem. Phys.* **1986**, *84*, 5465. (b) King, H. F.; Komornicki, A. In *Geometrical Derivatives of Energy Surfaces and Molecular Properties* Jorgenson, P., Simons, J., Eds.; NATO ASI Series C 166; D. Reidel: Dordrecht, The Netherlands 1986; p 207.

(24) Breidung, J.; Thiel, W.; Komornicki, A. *Chem. Phys. Lett.* **1988**, *153*, 76.

(25) GRADSCF is an ab initio program system designed and written by A. Komornicki at Polyatomics Research.

(26) Marsden, C. J. *J. Chem. Phys.* **1987**, *87*, 6626.

Table VI. Comparison of Observed and Calculated Frequencies of the Isoelectronic $TeOF_6^{2-}$ and IOF_6^- Anions, Together With Approximate Mode Descriptions

assignment (C_{5v})		approx mode description	$TeOF_6^{2-}$ obsd freq, cm^{-1} (intens (IR, Raman))	$TeOF_6^{2-}$ calcd freq,[a] cm^{-1}, (IR intens)	IOF_6^- obsd freq,[a] cm^{-1} (intens (IR, Raman))	IOF_6^- calcd freq,[b] cm^{-1}
A_1	ν_1	$\nu(X{=}O)$	830 (s, 71)	829.7 (122)	873 (vs, 53*p*)[e]	873
	ν_2	$\nu(X\text{–}F_{ax})$	614 (m, 100)	629.6 (73)	649 (s, 88*p*)	639.6
	ν_3	$\nu_{sym}(XF_5)$	530 (..., 80)	527.1 (0.1)	584 (*c*, 100*p*)	579.9
	ν_4	$\delta_{umbrella}(XF_5)$	330 (s, ...)	337.9 (104)	359 (s, 4)	363.0
E_1	ν_5	$\nu_{asym}(XF_5)$	525 (vs, ...)	529.9 (202)	585 (*v*s, *d*)	597.7
	ν_6	$\delta_{asym}(XF_5)$ in-plane	365 (vs, ...)	368.3 (272)	405 (*v*s, ...)	406.6
	ν_7	$\delta_{rock}(O{=}X\text{—}F_{ax})$	322 (..., 60)	314.6 (0.1)	341 (..., 62)	333.2
	ν_8	$\delta_{sciss}(O{=}X\text{—}F_{ax})$	245 (..., 2)	244.1 (1.3)	260 (s, 2)	267.4
E_2	ν_9	$\delta_{sciss}(XF_5)$ in plane	459 (w, 25)	456.7 (0)	530 (..., 4)	519.8
	ν_{10}	$\nu_{asym}(XF_5)$	388 (..., 35)	377.4 (0)	457 (..., 49)	457.3
	ν_{11}	$\delta_{pucker}(XF_5)$	not obsd	129.6 (0)	not obsd	138.1

[a] Frequency values were scaled by the following empirical factors to give the best fit with the observed frequencies: stretching modes, 0.9747; deformation modes, 0.8789. [b] The following empirical scaling factors were used: stretching modes, 0.9262 except for ν_1 = 1.0146; deformation modes, 0.8863. The values previously published in ref 15 are slightly different due to the use of a common scaling factor for both the stretching and the deformation modes. [c] Very strong IR band at 585 cm^{-1} is due to ν_5 and not ν_3, which should be of vanishingly small IR intensity. [d] Very strong Raman band at 584 cm^{-1} is due to ν_3 and not ν_5, which should be of vanishingly small Raman intensity. [e] *p* = polarized.

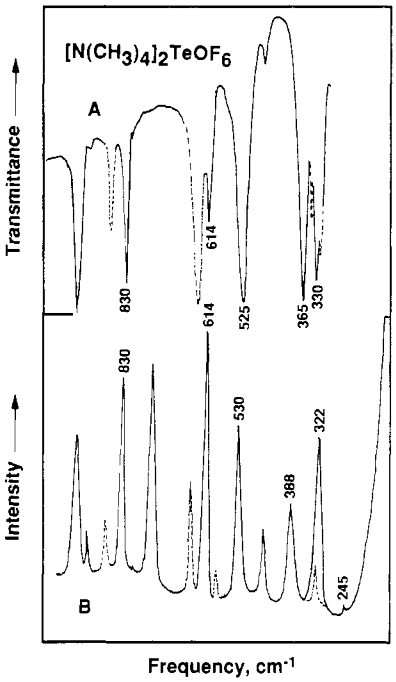

Figure 2. Infrared (A) and Raman (B) spectra of solid $[N(CH_3)_4]_2TeOF_6$. The dashed lines are due to $TeOF_5^-$.

by the bond lengths than the stretching modes, it is advantageous to use two different scaling factors for the stretching and the deformation modes.[26]

Results and Discussion

Synthesis and Properties of $[N(CH_3)_4]_2TeOF_6$. This compound was prepared according to

$$N(CH_3)_4TeOF_5 + N(CH_3)_4F \xrightarrow{CH_3CN} [N(CH_3)_4]_2TeOF_6 \tag{1}$$

Since both starting materials are soluble in CH_3CN while the desired product is not, the latter can easily be isolated by filtration or decantation. In spite of using a 2-fold excess of $N(CH_3)_4F$, the reaction product always contained some unreacted $TeOF_5^-$ salt as detected by vibrational spectroscopy. Since the dry $[N(CH_3)_4]_2TeOF_6$ salt is thermally stable at room temperature, the observation of some unreacted $N(CH_3)_4TeOF_5$ in the product implies that reaction 1 might be an equilibrium which is only incompletely shifted to the right. Attempts were made to remove the unreacted $N(CH_3)_4TeOF_5$ from the reaction product by repeated extractions with CH_3CN. Although the purity of the product was substantially improved in this manner, we did not succeed in the preparation of totally pure $[N(CH_3)_4]_2TeOF_6$.

Table VII. Scaled ab Initio Force Field[a,b] and Potential Energy Distribution of $TeOF_6^{2-}$

			sym force consts	PED
A_1	ν_1	829.7	$F_{11} = 5.727$ $F_{12} = 0.020$ $F_{13} = 0.190$ $F_{14} = -0.213$	91.3 (S_1) + 4.6 (S_2) + 4.0 (S_4)
	ν_2	629.6	$F_{22} = 3.811$ $F_{23} = 0.403$ $F_{24} = 0.362$	78.3 (S_2) + 18.0 (S_3) + 2.3 (S_4) + 1.4 (S_1)
	ν_3	527.1	$F_{33} = 3.335$ $F_{34} = 0.086$	80.0 (S_3) + 19.5 (S_2)
	ν_4	337.9	$F_{44} = 1.525$	100 (S_4)
E_1	ν_5	529.9	$F_{55} = 2.549$ $F_{56} = -0.997$ $F_{57} = 0.269$ $F_{58} = 0.239$	99.3 (S_5)
	ν_6	368.3	$F_{66} = 2.665$ $F_{67} = -0.226$ $F_{68} = -0.275$	33.0 (S_6) + 36.1 (S_8) + 18.1 (S_7) + 12.8 (S_5)
	ν_7	314.6	$F_{77} = 0.937$ $F_{78} = 0.074$	44.5 (S_7) + 54.4 (S_8)[c]
	ν_8	244.1	$F_{88} = 0.825$	34.2 (S_8) + 43.8 (S_7) + 21.3 (S_6)[d]
E_2	ν_9	456.7	$F_{99} = 2.306$ $F_{9,10} = 0.380$ $F_{9,11} = -0.065$	87.8 (S_9) + 12.2 (S_2)
	ν_{10}	377.4	$F_{10,10} = 1.742$ $F_{10,11} = -0.058$	88.6 (S_{10}) + 11.3 (S_9)
	ν_{11}	129.6	$F_{11,11} = 0.356$	99.9 (S_{11})

[a] The following scaling factors were used: stretching force constants, $(0.9747)^2$; deformation constants, $(0.8789)^2$; stretch–bend interactions, 0.9747 × 0.8789. Stretching constants were in mdyn/Å, deformation constants in mdynÅ/rad^2, and stretch–bend interaction constants in mdyn/rad. [b] The symmetry coordinates used were identical to those previously published in ref 15 for IOF_6^-. [c] Antisymmetric combination of S_7 and S_8. [d] Symmetric combination of S_7 and S_8.

Since $[N(CH_3)_4]_2TeOF_6$ has very little solubility in CH_3CN, single crystals for a crystal structure determination could not be grown. The ^{19}F NMR spectrum of $[N(CH_3)_4]_2TeOF_6$ in CH_3CN at −10 °C displays only weak resonances attributable to $TeOF_5^-$[$\delta(^{19}F_A)$, −19.1 ppm; $\delta(^{19}F_B)$, −36.9 ppm; $^2J(F_A - F_B)$, 170 Hz] and F^-[$\delta(^{19}F)$, −70.1 pm] but none assignable to $TeOF_6^{2-}$. When the temperature to is rasied 25 °C, rapid dissociation of the $TeOF_6^{2-}$ anion into $TeOF_5^-$ and F^- results in solvent attack by F^- and formation of HF_2^-.[27] Similar behavior has been noted previously[13] for $[N(CH_3)_4]_2TeF_8$ in CH_3CN, thereby demon-

---

(27) Christe, K. O.; Wilson, W. W. *J. Fluorine Chem.* **1990**, *47*, 117.

(28) Christe, K. O.; Wilson, W. W.; Bau, R.; Bunte, S. W. *J. Am. Chem. Soc.* **1992**, *114*, 3411 and references cited therein.

strating the strong propensity of these dinegative anions to dissociate in solution. As a consequence of the insolubility and instability of $[N(CH_3)_4]_2TeOF_6$ in CH_3CN, the recording of a ^{125}Te NMR spectrum for the $TeOF_6^{2-}$ anion has also not been possible. Consequently, the characterization of the $TeOF_6^{2-}$ anion was based entirely on its vibrational spectra and their comparison with those of the isoelectronic IOF_6^- anion whose structure has been firmly established by X-ray diffraction and NMR spectroscopy.[9] Since the samples of $[N(CH_3)_4]_2TeOF_6$ used for the spectroscopic study always contained some $TeOF_5^-$, it was necessary to first analyze the vibrational spectra of $N(CH_3)_4TeOF_5$.

Vibrational Spectra of $N(CH_3)_4TeOF_5$. The vibrational spectra of $N(CH_3)_4TeOF_5$ are shown in Figure 1 and the observed frequencies, together with their assignments, are summarized in Table I. The assignments for the $N(CH_3)_4^+$ cation follow those previously given[15,17,28] for other $N(CH_3)_4^+$ salts and, therefore, require no further discussion. The bands observed for the $TeOF_5^-$ anion are in general agreement with those previously reported[29–32] for the Cs^+, Ag^+, $[N(n\text{-}C_4H_9)_4^+]$, and 1,8 bis (dimethylamino)-naphthalenium salts. The previous assignments and normal coordinate analyses,[30,32] however, require substantial revision as shown by the results of our ab initio calculations (see Tables II–IV). In the previous studies ν_4, ν_5, ν_6, ν_7, ν_9, and ν_{11} had been incorrectly assigned. Our revised assignments are further supported by ^{16}O–^{18}O isotopic shifts[32] and calculated infrared intensities (see Table II). These results demonstrate again[12,15] the great benefit of reliable ab initio calculations for the correct analysis of vibrational spectra complicated by coincidences and low intensities of some of their bands.

Vibrational Spectra of $[N(CH_3)_4]_2TeOF_6$. The vibrational spectra of $[N(CH_3)_4]_2TeOF_6$ are shown in Figure 2 and the observed frequencies, together with their assignments, are summarized in Table V. Since the $TeOF_6^{2-}$ anion readily loses an F^- ion, it was not possible to obtain spectra which were completely free of $TeOF_5^-$ impurities. The bands due to $TeOF_5^-$ have been indicated in Figure 2 by dashed lines, and those due to $TeOF_6^{2-}$ have been marked by their frequency values. The unmarked bands belong to the $N(CH_3)_4^+$ cations.

Since the low solubility of $[N(CH_3)_4]_2TeOF_6$ preempted its characterization by NMR spectroscopy or single-crystal X-ray diffraction, a thorough vibrational analysis was carried out to establish the presence of the novel $TeOF_6^{2-}$ anion. As can be seen from Table VI, the vibrational spectra of $TeOF_6^{2-}$ are in excellent agreement with those of isoelectronic IOF_6^- and our results from ab initio ECP calculations. With the exception of the equatorial TeF_5 puckering mode, ν_{11}, which is difficult to detect because of its low intensity and frequency, all fundamental vibrations expected for $TeOF_6^{2-}$ have been observed. The observed frequencies deviate only by an average of 6.6 cm^{-1} from the scaled calculated frequencies, and the observed qualitative infrared intensities are in complete accord with the calculated values. The symmetry force constants and potential energy distribution (see Table VII), the internal stretching force constants (see Table VIII), the calculated geometry (see Table IX), and the total charge distribution (see Table X) are analogous to those[15] of isoelectronic IOF_6^-. As expected, the additional negative charge in $TeOF_6^{2-}$ increases the central atom ($\delta+$)–ligand ($\delta-$) bond polarities which can, at least partially, account for the lengthening of the bonds and the decrease in the values of the force constants. Interestingly, the equatorial Te–F stretching force constant decreases and the corresponding bond length increases by a much larger percentage than those of the axial bonds. This is not surprising in view of the bonding scheme previously proposed[15] for IOF_6^-. This scheme assumes a semiionic 6-center–10-electron bond system for the equatorial ligands. Therefore, these bonds should be more strongly influenced by the increased ionicity. Since the relationships between either bond lengths or force constants and atomic charges are strongly nonlinear and, at a −1.0 charge on fluorine, complete ionization and bond separation should occur, the changes in the atomic charges of such highly negatively charged fluorine ligands (see Table X) should not be expected to be proportional to those in the force constants or bond lengths.

Table VIII. Internal Stretching Force Constants (mdyn/Å)[a] of $TeOF_6^{2-}$ Compared to Those of IOF_6^-

	IOF_6^-	$TeOF_6^{2-}$	% change
fXO	6.256	5.727	−8.5
fXF$_{ax}$	4.095	3.811	−6.9
fXF$_{eq}$	3.086	2.383	−22.8

[a] Calculated ab initio ECP values scaled by the square of the scaling factors given in the footnotes of Table VI. The values given for IOF_6^- deviate somewhat from those of ref 15 due to the different scaling procedure (separate scaling of stretching and deformation modes) used to conform with those used for $TeOF_6^{2-}$.

Table IX. Calculated Geometry of $TeOF_6^{2-}$ Compared to the Calculated and Experimental Geometries of Isoelectronic IOF_6^-

		IOF_6^- [a]	
	$TeOF_6^{2-}$ calcd	calcd	exptl
r(X–O), Å	1.7598	1.7255	1.75–1.77
r(X–F$_{ax}$), Å	1.8400	1.8087	1.82
r(X–F$_{eq}$), Å	1.9373	1.8819	1.88
∠(OXF$_{eq}$), deg	95.9922	95.76	94–96

[a] Values from ref 15.

Table X. Total Charge Distributions for IOF_6^- and $TeOF_6^{2-}$

	IOF_6^- [a]	$TeOF_6^{2-}$		IOF_6^- [a]	$TeOF_6^{2-}$
central atom	2.71	2.88	F_{ax}	−0.44	−0.60
F_{eq}	−0.53	−0.66	O_{ax}	−0.74	−0.97

[a] Values from ref 15.

In summary, the vibrational spectra observed for the adduct between $N(CH_3)_4F$ and $N(CH_3)_4TeOF_5$ and their thorough analysis firmly establish the presence of the new $TeOF_6^{2-}$ anion and show that its structure and bonding closely resemble those found[15] for IOF_6^-.

Acknowledgment. The work at Rocketdyne was financially supported by the U.S. Air Force Phillips Laboratory and the U.S. Army Research Office, and that at McMaster University, by the U.S. Air Force Phillips Laboratory and the Natural Sciences and Engineering Research Council of Canada.

---

(29) Sladky, F.; Kropshofer, H.; Leitzke, O.; Peringer, P. *J. Inorg. Nucl. Chem. Suppl.* **1976**, 69.
(30) Mayer, E.; Sladky, F. *Inorg. Chem.* **1975**, *14*, 589.
(31) Thrasher, J. S.; Seppelt, K. *Z. Anorg. Allg. Chem.* **1985**, *529*, 85.
(32) (a) Strauss, S. H.; Abney, K. D.; Anderson, O. P. *Inorg. Chem.* **1986**, *25*, 2806. (b) Miller, P. K.; Abney, K. D.; Rappé, A. K.; Anderson, O. P.; Strauss, S. H. *Inorg. Chem.* **1988**, *27*, 2255.